The Thesis Committee for Mengqi Yuan
Certifies that this is the approved version of the following thesis:

Thermal Conductivity Measurements of Polyamide Powder

APPROVED BY
SUPERVISING COMMITTEE:

Supervisor:

David L. Bourell

Joseph J. Beaman Jr

Thermal Conductivity Measurements of Polyamide Powder

by

Mengqi Yuan, B. E

Thesis

Presented to the Faculty of the Graduate School of

The University of Texas at Austin

in Partial Fulfillment

of the Requirements

for the Degree of

Master of Science in Engineering

The University of Texas at Austin

December 2011

Acknowledgments

I would like to express my sincere gratitude to Dr. Bourell for being an extremely nice and motivating advisor. This thesis would not have been possible without his valuable support, assistance, guidance and encouragement. Deepest gratitude is also given to Tim Diller, who taught and helped me a lot during the research and to be more accustomed to American life style. I would like to thank Dr. Beaman for his advice and time spent in reading my thesis.

I would like to thank Mark Philips who nicely helped me in laser sintering process. I would also like to thank Rosalie Foster and David Justh for their excellent administrative skills.

My parents have always encouraged me to pursue my dreams and supported decisions. I would like to thank them and love them from the bottom of my soul and the depths of my heart.

I would like to thank Prof. Weicheng Fan and Prof. Hui Zhang for their kind help and warm-hearted guidance throughout my undergraduate and graduate study.

I want to thank my boyfriend Chengyang Yan for his constant love and strength. I could not finish this thesis without his support and encouragement. Many thanks are also given to my lovely roommates Yunping Fei and Maris Yan, who are always there when I need support.

Abstract

Thermal Conductivity Measurements of Polyamide Powder

Mengqi Yuan, M. S. E

The University of Texas at Austin, 2011

Supervisor: David L. Bourell

An important component in understanding the laser sintering process is knowledge of the thermal properties of the processed material. Thermal conductivity measurements of pure polyamide 12 and polyamide11 with multi-wall carbon nanotubes were conducted based on transient plane source technology using a Hot Disk® TPS500 conductivity measurement device. Polyamide powder was packed to three different densities in nitrogen at room temperature. Thermal diffusivity and conductivity were measured from 40°C to 170°C for both fresh powder and previously heated ("recycled") powder. The fresh powder tests revealed that thermal conductivity increased linearly with temperature whereas for previously heated powder, more constant and higher thermal conductivity was observed as it formed a powder cake. Tests were also performed on fully dense polyamide 12 to establish a baseline. Polyamide 12 powder had a room-temperature thermal conductivity of approximately 0.1 W/mK which

increased with temperature, whereas the bulk laser sintered polyamide 12 room-temperature value was 0.26 W/mK and generally decreased with increasing temperature.

Table of Contents

List of Figures

Chapter 1: *Introduction*

Chapter One includes a literature review of the laser sintering process, a thermal model that was built based on laser sintering, previous measurement of thermal conductivity in powder bed, theoretical calculation of thermal conductivity for powder beds, and the motivation for the present work.

REVIEW OF LS AND PA12

Laser sintering (LS) is an additive manufacturing technology that uses a high power laser to fuse polymer powder into a mass that has a desired 3-dimensional shape. Fig. 1 shows the process chain of the laser sintering process [1]. The laser selectively scans and fuses powder material layer-by-layer on the surface of the powder bed based on the previously generated CAD file, which is always industry-standard STL file format. After one layer is scanned, the powder bed is lowered by one layer thickness, creating a new layer that is scanned. The process is repeated until the part is completed.

Polyamide (PA) 12, also known as Nylon 12, is a thermoplastic material that widely is used in laser sintering. It has a high break elongation of 250 %, yield tensile elongation 20 %, flexural modulus 1590 MPa, flexural strength 60 MPa, notched Izod impact 5- 20 KJ/m^2 at 23 °C, good tensile strength (50 MPa), and melts at a temperature

around 180°C [2]. Thermal conductivity measurement of polyamide12 is essential to assessing the material performance during heating and cooling in laser sintering. Based on the material performance observed and samples produced, a more effective and accurate process control can be designed.

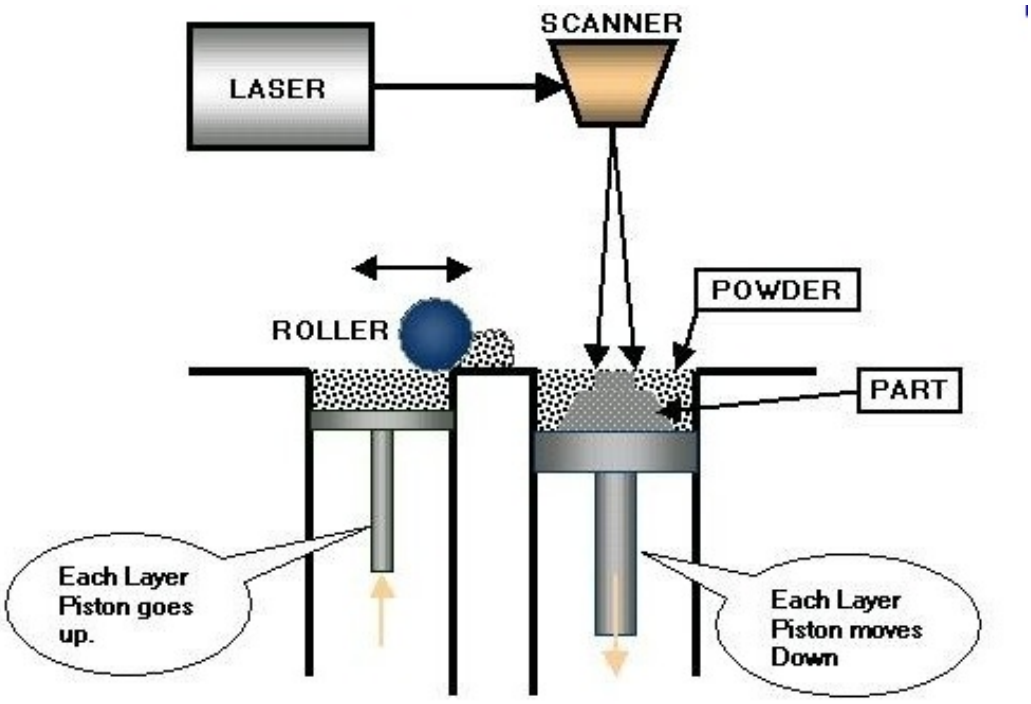

Figure 1: Schematic layout of laser sintering process

REVIEW OF THERMAL MODELS OF LS

Dressler *et al* [3] described the temperature distribution in the powder bed during the laser sintering printing process. A 1D transient model was applied to analyze the temperature distribution in the powder bed under different heating conditions and two powder types: a stainless steel and an apatite-like ceramic. Spectral emissivity of the powders were measured experimentally for wavelengths between 3 and 10 μm and used to determine the total radiative flux from a black body center. Thermal diffusivity was measured with a commercial hot-disk device. The powder surface was modeled as a combination of radiative - convective flux, while other boundaries were modeled as adiabatic. Computer results were compared to thermocouple measurements of the actual powder bed being modeled. However the calculation under predicted the thermal response times, so they predicted the expected differences due to the thermal diffusivity and emissivity. The thermocouple measurements were hindered due to the conductivity of the thermocouple wires and the participation of the thermocouple in radiative heat transfer at the surface.

M. Matsumoto *et al* [4] suggested using a finite element method to calculate the distribution of temperature and stress within a single layer of the powder bed in the laser sintering process. Plane stress deformation was applied on the solidified part, and a two dimensional finite element method for heat conduction and elastic deformation was incorporated. The finite element mesh was constructed on the surface layer of the powder bed in the simulation. Heat caused by the laser was applied to the elements under the laser beam. Shrinkage due to solidification was assumed, leading only a change of the layer thickness. The deformation and tensile stress distribution result presented the possibility and location of the layer forming cracking, and the amount of the solid layer deflection increased with the track size increment. So a shortened scanning track is preferred to prevent the distortion of the solid layer on the powder bed.

S. Kolossov *et al.* [5] built a 3D thermal mode based on continuous media theory using finite element analysis. The laser radiation is considered as the heat source and penetrates a certain distance from the surface into the bed, which is called 'penetration depth' and dependent on the material properties. The geometry of the radiation is defined by the absorption phenomena from the surface layer. The laser sintering process was analyzed as a three-dimensional, non-linear heat transfer problem with no volume heat source. Their model proved the evolution of the thermal conductivity occurred at temperature higher than the threshold temperature and it remained low in the regions of

lower temperature. A thermal conductivity jump could only be compensated by a temperature gradient jump in order to ensure heat flux continuity. A non-linear behavior analysis of thermal conductivity and specific heat was conducted as a result of the temperature change and phase transformation. Thermal conductivity of the bulk solid titanium decreased from 0 °C (22.5 W/mK) to 300°C (19.5 W/mK), and then increased to 28W/mK at 1600°C. The model with constant thermal conductivity failed to produce the real temperature pattern. The results indicated that sintering behavior was strongly influenced by thermal conductivity on a titanium powder bed, and thermal conductivity was very sensitive parameter that had to be computed by taking the thermal history into account.

Rahul *et al.* [6] used transient finite element methods to build a thermal model to analysis temperature distribution in single metal powder layer in metal laser sintering process and assumed the powder layer subjected to plane stress type of temperature variation. Several assumptions were made including the input heat flux caused by laser irradiation was regarded as an internal heat generation in the powder layer and fully covered by the finite element under the laser beam, the part temperature that equal or higher than melting temperature was assumed to be sintered, and so on. The top surface temperature during the experiment that measured was 1500 K and calculated as 2134.8K from this FEM model. In terms of the temperature distribution in the powder

layer, it gradually decreased on both sides of laser center. There was an increase in temperature with increasing laser power that was changed between 2W and 4 W in 1W increments. The temperature gradient along the *X*-axis increased from 6.9 to 9.5 K/m and 7.4 to 10.1 K/m along *Y*-axis. In addition, the heat flux given to the powder layer increased with increasing laser powder. The peak temperature was observed not exactly at the laser beam center but slightly decreased on position on *X*-axis and increased on *Y*-axis. The powder bed temperature increased with the increasing beam dimension, but after the beam diameter reached 0.15 mm, the temperature decreased constantly. Moreover, the powder bed temperature increased with the increasing laser on time and decreased with the increasing laser off time.

Tolochko *et al* [7] investigated sintering and heat transfer mechanisms in Ti powder using numerical simulations. Loose powders consisted of spherical particles and irregular shapes. 10-mm-thick powder layers were put on Al substrates that were assumed to have no impact on the processing zone. The simulation results of the temperature and neck size distributions of the sintered samples were in good agreement with the experimental results, which presented a hemispherical temperature profile from the laser spot. The model predicted the laser power which caused the remelting process (approximately 60W) as well. Detectable sintering started when the α- Ti was changed to β- Ti, which was controlled by contact thermal conduction and constituted the largest

portion of the powder bed during the sintering process. The radiative thermal conduction dominated the heat transfer by determining the temperature propagation speed through the powder bed. Both simulation and experimental results suggested that the sample consisted of a remelted core and a low-sintered zone with a relative neck size around 100 μm. The increment of the volumetric specific heat with the density contributed most to the part build, comparing to the increasing of the radiative thermal conductivity with the particle size and the increasing of the contact thermal conductivity with the powder density. In addition, the model correctly described the variations of the sintered samples and sintered domain dimensions with the laser power and the powder type.

PREVIOUS MEASUREMENTS OF THERMAL CONDUCTIVITY IN POWDER

There are limited experimental results for thermal conductivity of polyamide powders, but some exist for other powders, including metal and ceramic powder.

To understand the material behavior during the laser sintering process, there is a basic relation that combines a material physical property with thermal properties:

$$\alpha = \frac{k}{\rho c} \tag{1}$$

where α is thermal diffusivity, k is thermal conductivity, ρ is the sample density, and c is the specific heat.

Saxena, Chohan and Gustafsson's model [8] treated the natural loose and granular materials as a solid-gas mixture; neither phase provided a continuous medium. The thermal conductivity calculation was separated according to the porosity level:

$$k = k_{ec}\,(1+3.844(0.5-\varepsilon)^{2/3}) \quad \text{when } \varepsilon < 0.5 \tag{2}$$

$$k = k_{ec}\,(1-1.545(\varepsilon-0.5)^{2/3}) \quad \text{when } \varepsilon > 0.5 \tag{3}$$

$$k_{ec} = 0.6132(k_a k_s)^{1/2} \tag{4}$$

where k_{ec} is the thermal conductivity of the effective continuous medium, k_a and k_s are the thermal conductivity of the air and solid at the same temperature, ε is the relative porosity. This method required obtaining all the thermal conductivities in advance, without knowing any other thermal properties, including thermal diffusivity, specific heat and temperature, which are essentially related to the thermal conductivity. However, the advantage of this method is it includes the porosity which influences the thermal effect significantly.

Samuel Xue and J. W Barlow [9] made measurements on several powders, including ABS, PVC, nylon, and wax. Thermal conductivity was measured by filling a thin-walled aluminum cylinder with power at a uniform initial temperature T_0. The

cylinder was immersed in a constant temperature bath at T_∞. Time response of the centerline temperature T_c was measured by a thermocouple. A theoretical solution of the centerline temperature variation was given by:

$$T_c = T_\infty - (T_\infty - T_0)\, B_1\, e^{\frac{B_2 \alpha t}{R^2}} \qquad (5)$$

where B_1 and B_2 were calculated by geometry: $B_1 = 1.6$, $B_2 = -5.8$. Thermal diffusivity was obtained by rearranging equation (5) and fitting the observed temperatures.

They found that the thermal conductivity of powder generally increased with increasing temperature. However, the shape of the thermal conductivity versus time curves can be quite different for the varying materials. For an unspecified nylon powder:

$$k = -2.2139 + 0.020569T - 0.000062289T^2 + 0.000000063221T^3 \qquad (6)$$

where k is in W/mK, T is the absolute temperature in K from 280-360 K. It gives a thermal conductivity around 0.0604 ~0.0679 W/mK from 40°C to 87°C. The value of this prediction is limited due to the limited temperature range, lack of information relating to material and experimental conditions, and sample preparation.

Dressler *et al* [10] reported the temperature distribution in metal and ceramic powder beds during three-dimensional printing. Both powders were characterized in terms of thermal conductivity, diffusivity, emissivity, and density. Thermocouple was

implanted into the print bed to measure the temperature distribution in the powder bed and a commercial transient plane source instrument was used to measure the thermal conductivity of metal and ceramic powders. They found that the temperature in the powder bed increased linearly with the heater power and the ceramic powder heated up and cooled down quicker than metal powder. Moreover, low thermal conductivities were found for metal and ceramic powders, which were 0.19 and 0.14 W/mK, due to the low packing density.

Fischer *et al* [11] built an interaction model for near infrared laser pulses with different metal in laser sintering. They established a set of thermal conductivity data on Ti, Ni, WC-12Co metal powders, which were 1.45, 1.23, 1.46 W/mK respectively. The bulk material thermal conductivities were much higher from 20 W/mK for Ti, 80 W/mK for WC- 12Co and 90 W/mK for Ni. However, they did not mention the measuring temperature and powder density for each metal powder thermal conductivity measurement.

Deissler-Boegli Model [12] showed that the effective thermal conductivity of powder was a function of the conductivity of the gas, and was nearly independent of pressure. For example, the effective conductivity of magnesium oxide powder in helium was about five times that for the same powder in argon.

THEORETICAL CALCULATIONS OF THERMAL CONDUCTIVITY FOR POWDER BEDS

Deissler and Boegli [12] described the condition of the maximum and minimum effective thermal conductivity k_{ef} of a two phase system (gas and solid): the maximum k_{ef} occurs when the material is arranged in alternating layers parallel to the flow of thermal energy, which means the contact resistance is ignored; while the minimum k_{ef} occurs when the material is arranged in alternating layers perpendicular to the flow of thermal energy, which means the contact resistance reaches the maximum. Equations (7) and (8) indicate these two conditions separately:

$$\frac{k_{ef}}{k_g} = \varepsilon + \frac{k_s}{k_g}(1-\varepsilon) \qquad \text{[maximum]} \qquad (7)$$

$$\frac{k_{ef}}{k_g} = \frac{1}{\varepsilon + \frac{1-\varepsilon}{k_s/k_g}} \qquad \text{[minimum]} \qquad (8)$$

where k_s is the thermal conductivity of the solid, k_g is the thermal conductivity of the gas, ε is the relative porosity, k_{ef} is the maximum or minimum effective thermal conductivity.

The porosity-based method is appropriate for powder beds in that the thermal conductivity varies with porosity, which would influence the laser sintering process and the bulk material produced. However, this approach assumes good thermal contact and is not suitable for unsintered powders.

Gusarov *et al* [13] estimated contact thermal conductivity in laser sintering using a model concluded independent small thermal contacts based on the coordination number and the contact size. The contact size was assumed small compared to the particle size, the radius ratio falling below 0.3. The effective thermal conductivity was proportional to the contact size but the proportionality factor was strongly dependent on the structure type. Moreover, at a given contact size, the effective thermal conductivity increased with the sample density and the coordination number.

Slavin *et al.* [14] measured the thermal conductivity of an uncompressed powder bed considered the surface roughness of the spheroids, which was measured by a profilometer. The thermal conductivity for the 3-mm Al spheroids increased from 1 to 1.6 W/mK from 300 K to 850 K, while thermal conductivity for the 1-mm Al spheroids increased from about 0.8 to 1.5 W/mK from 300 K to 850 K. The particle roughness was found to be essential by determining the average separation of the particles, which controlled the gaseous contribution to the powder bed thermal conductivity.

Slavin *et al* [15] analyzed the effective thermal conductivity of packed beds of solid alumina spheroids in helium at 100 to 500°C up to 100 KPa pressure. Two fitting factors were considered in 1 mm and 3 mm nominal diameter solid alumina spheroids: the width and the average radius of the narrow gaps that existed between the irregularly shaped particles. Results showed that the effective thermal conductivity increased with temperature changing from 400K to 700K. However, too many parameters were involved within this model, which made the experimental uncertainty high.

Polyamide is an essential material in the laser sintering process. However, limited experimental data for thermal conductivity of polyamide powder exists in the published literature and most of them did not mention the measurement temperature nor measured at room temperature. Therefore, thermal conductivity measurements of polyamide and polyamide nanocomposites were conducted and analyzed in this thesis.

Chapter 2: *Experiment Procedure*

Chapter two includes two parts: a description of thermal conductivity measurements, which describes the TPS 500 apparatus for measuring different samples; and a description of bulk sample density measurements, which used a helium pycnometer to measure the polyamide 12 cylinder density.

THERMAL CONDUCTIVITY MEASUREMENT

Apparatus

A plane-source transient thermal conductivity measurement machine (HotDisk® TPS 500) and a temperature control oven were acquired, which are shown in Fig. 2. A powder holder was fabricated, allowing the conductivity probe to be sandwiched between the two sections of powder. The interstitial gas was heated through the copper tubes that were hung on the inside wall.

In each experiment, a direct current that was large enough to increase the sensor temperature by 1-2 K passed through the sensor. The sensor resistance changed which resulted in a voltage drop. A precise relation of the heat flow between the sensor and the test specimen was obtained by the transient response in the polyamide powder.

According to the heat flow and the geometric information, specific heat and thermal diffusivity were obtained by the Hot Disk software. Due to the basic relation: $k=\alpha*\rho*c$, the thermal conductivity could be obtained [16]. Here, α is the thermal diffusivity, ρ is the density and c is the specific heat.

The powder (Duraform® PA, a 50 μm polyamide -12 powder) was loaded into the sample holder and tapped to settle it before the measurement.

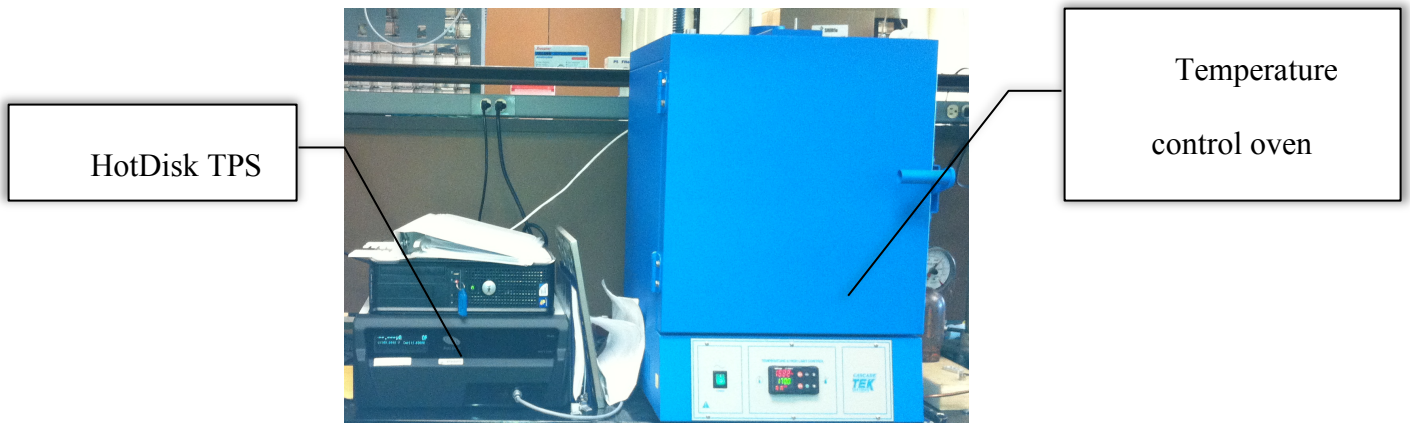

Figure 2: Commercial thermal conductivity measuring device TPS 500 and temperature control oven.

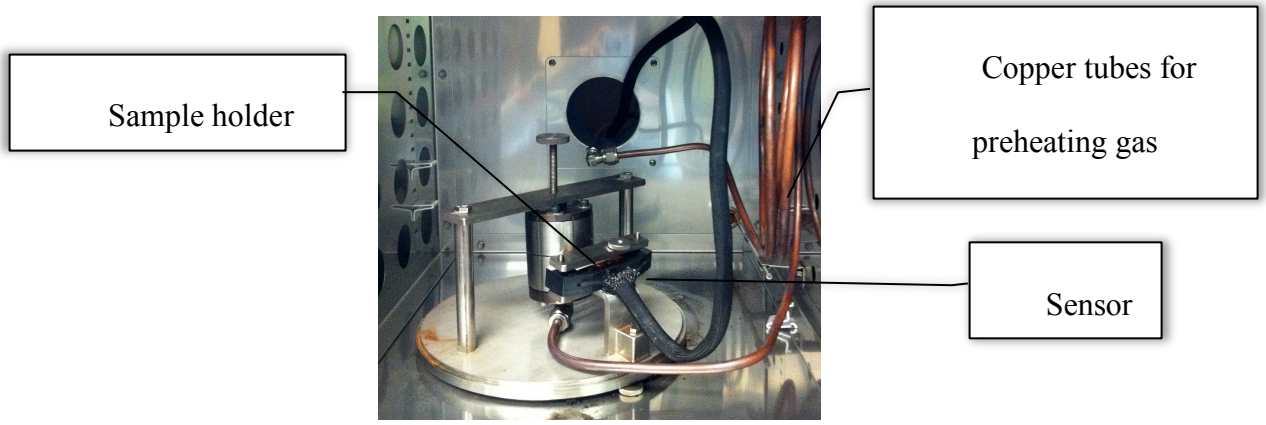

Figure 3: Experimental apparatus for measuring the thermal conductivity of polyamide-12 powder. The view is inside the temperature control oven, which includes the sample holder, copper tubes and sensor.

Procedure

According to Mark's Handbook [17], polyamide 12 powder has a melting temperature approximately 180°C. For this reason, 170°C was selected as the highest test temperature. During experimental runs, a 10°C increment was selected. Interstitial gas-N_2 (purity 99.95%) was purged by adding an inlet port at the bottom, and a diffuser port at the top. This construction was used to prevent oxidation and to boost the heating process.

The specific heats at three typical temperatures: 300 K, 400 K and, 600 K were obtained from Mark's Handbook [14]. Xue's paper established a linear relation on specific heat of polyamide and temperature [7], so a relation was built:

$$C_p = (T\text{-}300)* \frac{(2.4709-1.6952)}{(100)} + 1.6952 \qquad [313\ K \leq T \leq 400\ K] \qquad (9)$$

$$C_p = (T\text{-}400)* \frac{(3.2786-2.4709)}{(200)} + 2.4709 \qquad [401\ K \leq T \leq 443\ K] \qquad (10)$$

To convert the standard C_p mass units (KJ/kg K) into volumetric units (MJ/m^3 K) that the TPS500 used for the thermal diffusivity calculation, the calculated specific heat was multiplied by the sample relative density.

The powder relative density was obtained by dividing the powder mass by the measured interior volume of the sample holder, which was 21,097 mm^3. Powder mass was obtained by measuring the weight difference from an empty beaker and the beaker with a sample after the experiment.

At each temperature, eight individual measurements were made, each of which lasted 80 seconds. Fifteen minutes separated each measurement, allowing the sample to reach a steady state. It took 2~3 hours to reach an equilibrium state at each temperature.

The heating power was 60 mW with an electrical frequency of 60 Hz. The sensor material was Kapton with a radius of 6.403 mm. The available probing depth was 12.00 mm.

The 80-second experiment time included a 40 s drift time and 40 s testing time. The measured sensor temperature before heating showed small variations, which indicated the equilibrium state. The transient graph shows the temperature increases 1-3 K. The first 50 points were ignored since the temperature increased too quickly in a short time, while 51-200 points were selected, which formed a smoothly increasing straight line. The drift graph was shown in Fig. 4 and the transient graph was shown in Fig. 5.

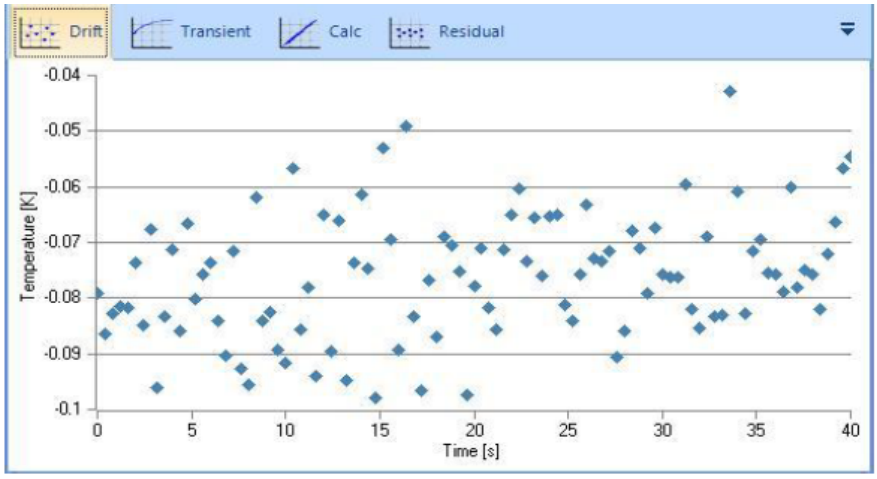

Figure 4: Drift graph shows small variation of temperature of polyamide 12 before heating that indicates a steady state before the experiment.

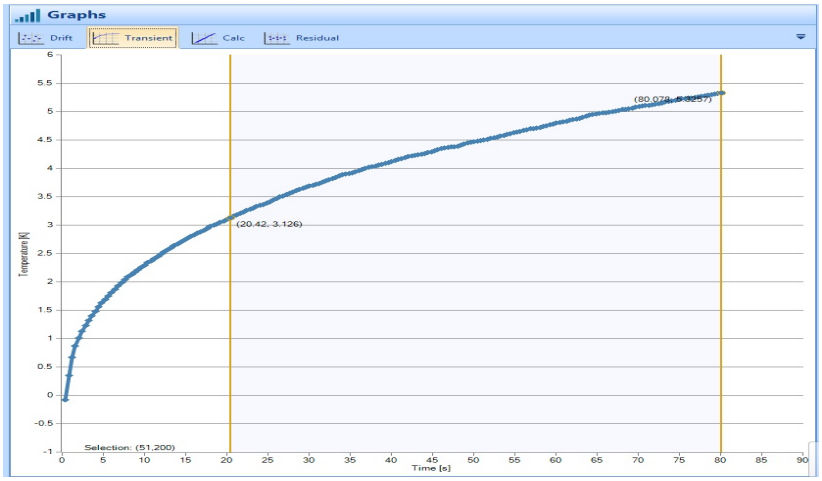

Figure 5: This transient graph shows the 1-3 K temperature increased of polyamide 12 during the thermal conductivity measurement. The blue smoothly increasing line between two yellow vertical lines presents a constant temperature increment during the experiment.

In terms of analyzing the effect of preheated powder, the experiments were conducted in the same manner from 40°C to 170°C after fresh powder was heated to 170°C and cooled down to room temperature.

To assess the effect of powder cake morphology in thermal conductivity measurement, fresh polyamide 12 powder was heated to 170°C and cooled down to

40°C at which point it became caked. Part cake was manually crushed back into powder, packed into the sample holder, and the experiment was repeated.

To analyze the temperature effect of powder caking on the thermal properties, a repeated experiment containing five runs was first performed at 40°C, 90°C and 140°C; second performed at 40°C, 90°C, 140°C, and 150°C; third performed at 40°C, 90°C, 140°C, 150°C, and 160°C; fourth performed at 40°C, 90°C, 140°C, 150°C, 160°C and 170°C; the last run repeated the fourth run again.

Different inert gases, nitrogen and argon, were purged during the steady-state portion of the thermal conductivity measurement to assess the influence of different carrier gases.

Finally, different loadings (0, 1, 3, 5, 7, 9 %) of multi-wall carbon nanotubes were incorporated into nylon 11 using a powder-powder mixing technique to obtain nanocomposite powder. Thermal conductivity measurements were carried at 40°C and 175°C, before cooling back to 40°C. The experiments were repeated.

BULK SAMPLE DENSITY MEASUREMENT

A Quantachrome INSTRUMENTS® ULTRAPYC 1200e helium pycnometer was used to measure the density of a fully dense polyamdie 12 bulk cylinder that was produced by laser sintering. Helium was chosen as a probe gas in that it features a very small atomic size and can permeate the narrow pores in a solid, permitting the determination of the real volume occupied by the sample [18]. An accurate polyamide 12 cylinder volume was obtained from the well known ideal gas law:

$$PV = NRT \qquad (11)$$

The mass was measured by a Denver INSTRUMENT® weightometer APX-200. The density of the polyamide 12 solid cylinder was calculated from $\rho = m/ V$.

Chapter 3: *Results*

Chapter three presents six factors that influence the thermal conductivity of polyamide, which includes density, virginity, temperature, geometry, carrier gas and multi-wall carbon nanotube loading.

EFFECT OF POWDER BEHAVIOR AT DIFFERENT DENSITY

The effect of powder packing density for fresh polyamide 12 powder is shown in Figure 6. It describes the fresh polyamide 12 thermal conductivity from 40 °C to 170 °C at three densities. The thermal conductivity increased linearly with increasing temperature. It also increased with packed density. Moreover, all thermal conductivities are within the range of 0.09 – 0.12 W/mK.

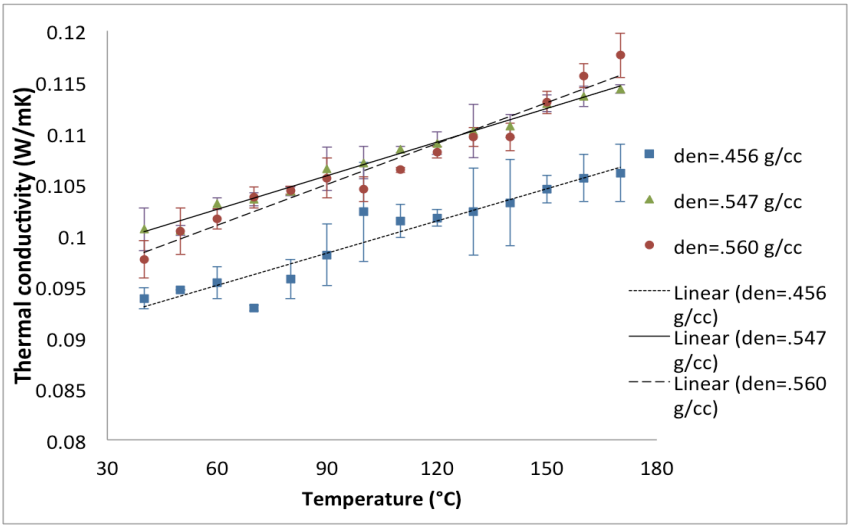

Figure 6: Temperature dependent thermal conductivity of fresh polyamide 12, initially packed at three densities: 0.456g/cc, 0.547g/cc, and 0.560g/cc. Each point on the graph is the mean value of five individual measurements.

A thermal conductivity comparison with bulk laser sintered polyamide 12 is in Figure 7. It shows that the bulk laser sintered polyamide 12 has a thermal conductivity around 0.22 ~ 0.30 W/mK from 40 °C to 170 °C with a density of 0.99 g/cc measured by Quantachrome INSTRUMENTS® ULTRAPYC 1200e helium pycnometer. This is much larger than loose polyamide 12 powder thermal conductivity. In addition, bulk material thermal conductivity presents a different trend from the loose- form thermal

conductivity. It increased to a maximum at 70 °C (0.28 W/ mK) than continually decreased with increasing temperature to 0.24 W/ mK.

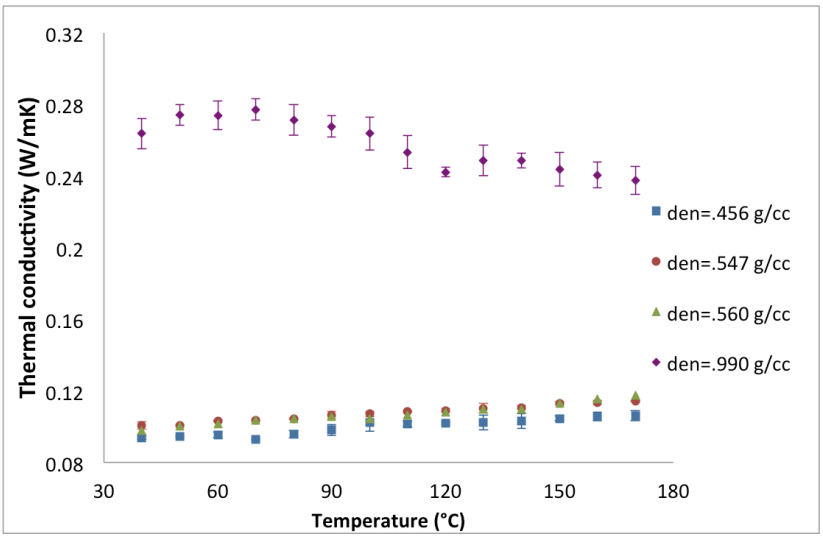

Figure 7: Temperature dependent thermal conductivity of loose polyamide 12 powder at three densities as compared to bulk laser sintered polyamide 12. Each point on the graph is the mean value of five individual measurements.

The thermal conductivities of previously heated to 170°C polyamide 12 powder at three packing densities are shown in Figure 8.

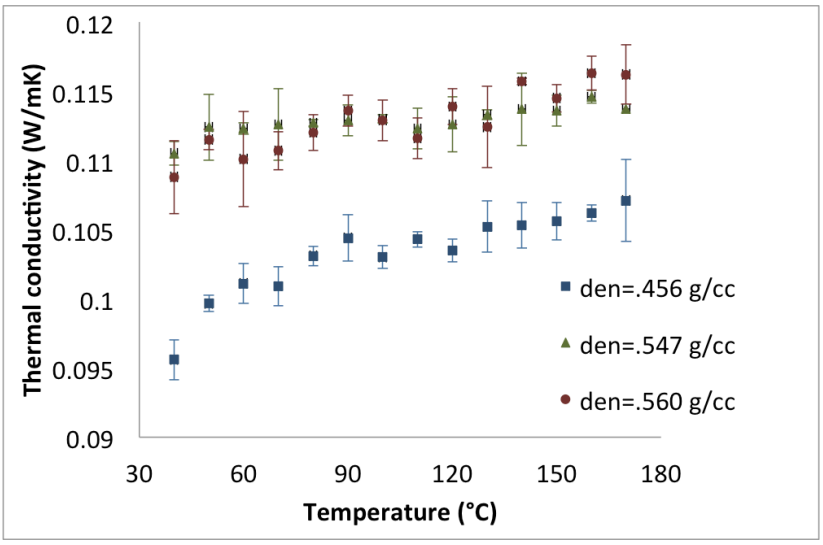

Figure 8：Temperature dependent thermal conductivity of polyamide 12 powder that was packed at three densities: 0.456g/cc, 0.547g/cc, and 0.560g/cc and heated to 170 °C cooled and then tested. Each point on the graph is the mean value of five individual measurements.

Figure 8 shows the thermal conductivity of polyamide 12 powder previously heated to 170 °C as a function of temperature. “Part cake” was formed at this stage. All data are within the range of 0.095 ~ 0.12 W/mK. Thermal conductivity evenly increased with increasing temperature and density. The thermal conductivity of powder packed at 0.547 g/cc is quite similar with that packed at 0.560 g/cc.

EFFECT OF PREHEATED POWDER

Figures 9-10 compare the thermal conductivity of fresh powder to powder previously heated to 170°C as functions of the three powder packing densities.

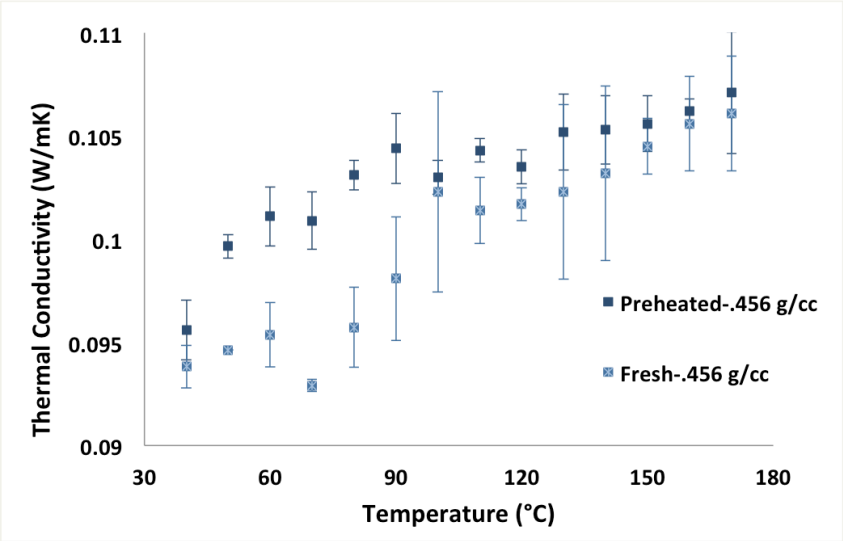

Figure 9：Thermal conductivity comparison between fresh polyamide 12 powder and polyamide 12 powder that previously heated to 170°C. The initial packing density was 0.456 g/cc.

Figure 9 compares the thermal conductivity of fresh powder and previously heated to 170°C powder (“part cake”) packed at 0.456 g/cc. Fresh powder shows a more linear

increasing trend than “part cake”. The thermal conductivity are all increased from 0.9 ~ 0.11 W/mK from 40 °C to 170°C.

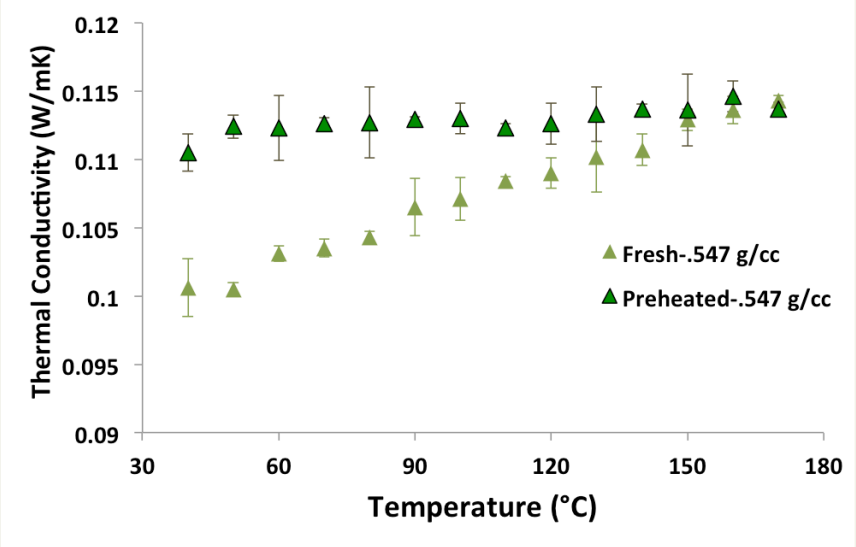

Figure 10：Thermal conductivity comparison between fresh polyamide 12 powder and polyamide 12 powder that previously heated to 170°C. The initial packing density was 0.547g/cc. The comparison at a density of 0.560 g/cc is similar with that at 0.547g/cc.

Figure 10 compares the thermal conductivity of fresh powder and previously heated to 170°C powder (“part cake”) packed at 0.547 g/cc. Fresh powder shows a much larger temperature dependence than “part cake”: the fresh powder thermal conductivity

increased from 0.1 W/ mK to 0.114 W/ mK, an increase of 0.014 W/ mK while the "part cake" thermal conductivity increased from 0.11 to 0.114 W/mK, which increased by only 0.004 W/ mK.

Figure 11 illustrates the effect of preheat to 170°C treatment on polyamide 12 loose powder that initially packed at 0.566 g/cc. It shows the results of an experiment which first measured thermal conductivity of fresh powder and previously heated to 170 °C polyamide 12 powder packed at 0.560 g/cc. Then the "part cake" was mechanically crushed back into loose powder form and the thermal conductivity was measured from 40 °C to 170 °C. The fresh powder thermal conductivity is similar to the crushed "part cake" thermal conductivity, which both increased linearly with increasing temperature from 0.96~ 0.102 W/mK at 40 °C to 0.114~ 0.118 W/ mK at 170°C. The "part cake" thermal conductivity increased evenly with temperature increasing from 0.11 W/mK to 0.118 W/mK.

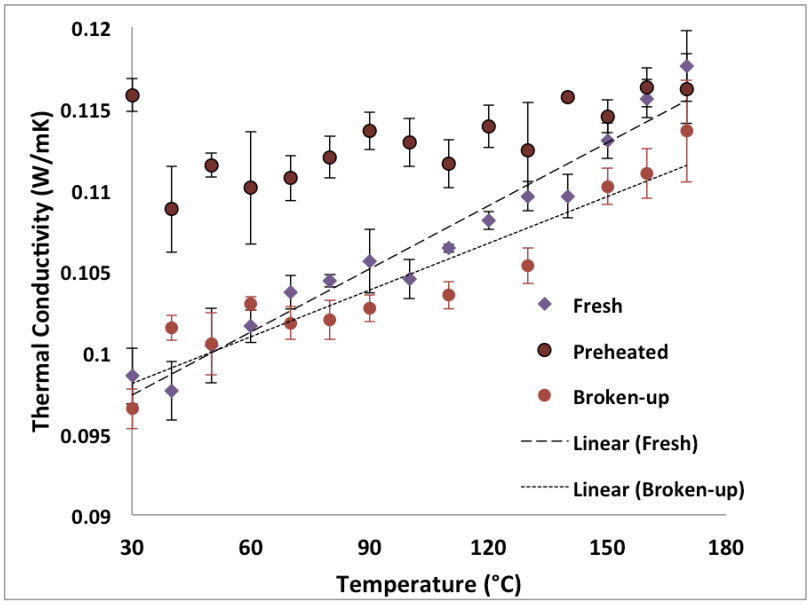

Figure 11：Thermal conductivity comparison between fresh polyamide 12 powder and polyamide 12 powder that was previously heated to 170°C. The initial packing density was 0.560 g/cc. Also shown is the change in thermal conductivity that occurs when the previously heated ("part cake") powder was mechanically crushed back into loose powder.

EFFECT OF TEMPERATURE ON POWDER CAKING

The effect of temperature on powder caking was analyzed by measuring the thermal conductivity from 140°C to incrementally higher temperatures and assessing the point at which the thermal conductivity increased upon cooling to room temperature.

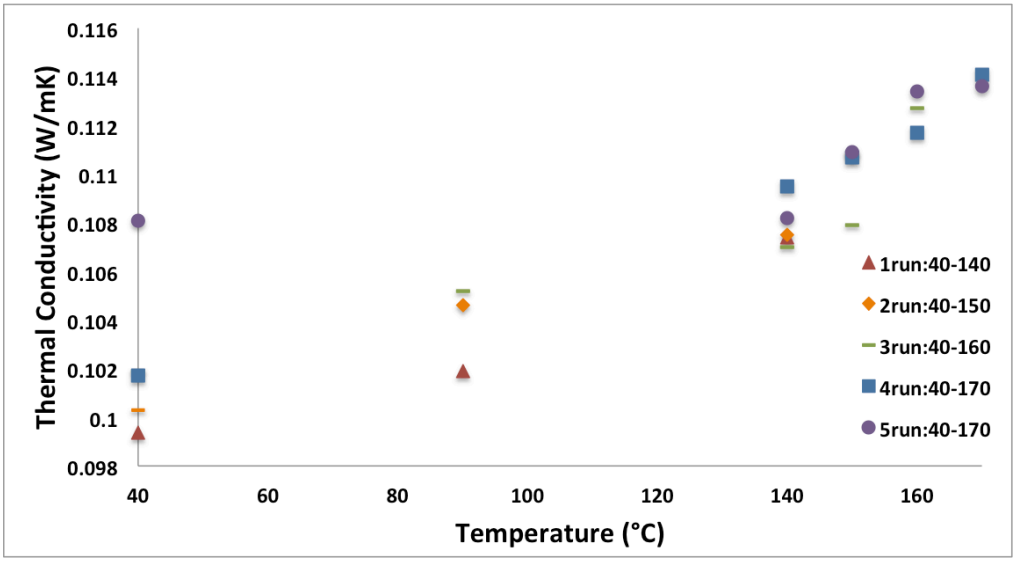

Figure 12： Polyamide 12 powder heated from 40°C to increasingly higher maximum temperatures before cooling. The powder initial relative density was 0.566 g/cc.

Figure 12 reveals the temperature effect on powder caking. The thermal conductivity increased linearly during the first four runs, which were all around 0.1 W/mK at 40°C; however it shows a more even increasing thermal conductivity during the last run, which was repeating the heating process from 40°C to 170°C. It shows a larger thermal conductivity at 40°C: 0.108 W/mK.

EFFECT OF CARRIER GAS

The effect of carrier gas was conducted by purging nitrogen or argon on the specimen at room temperature and during the heating process. The experiments were first run on fresh polyamide 12 powder and previously heated to 170°C polyamide 12 powder. The density of powder purged with nitrogen was quite close to that purged with argon, which made the two sets of results comparable. Figure 13 illustrates that the temperature dependent thermal conductivity did not change with the carrier gas change. However, the error bars for the four curves are large, which reduce the accuracy of experiment.

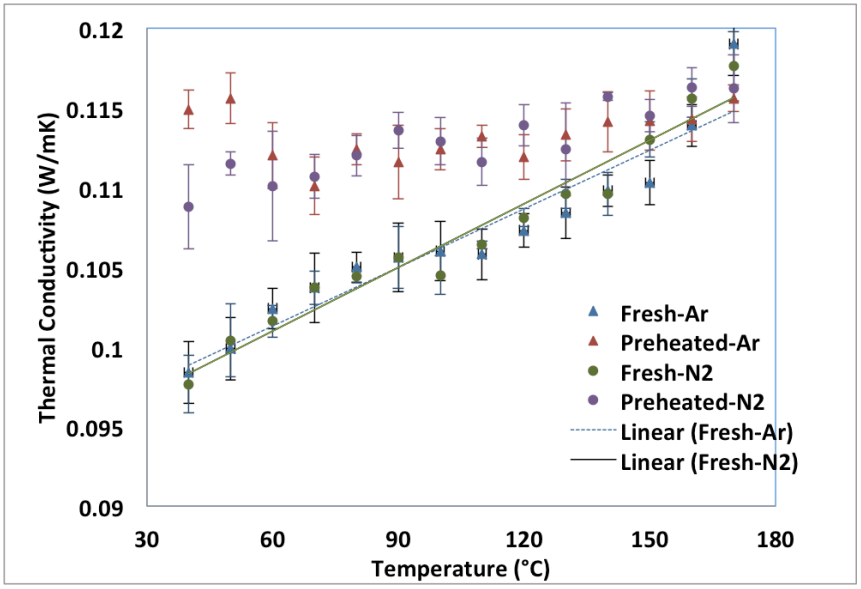

Figure 13: Polyamide 12 temperature dependent thermal conductivity measurement results of both fresh and previously heated to 170°C powder in nitrogen and argon environment. The powder initial relative density was 0.566g/cc.

EFFECT OF MWNT NANOCOMPSITES

Figures 14 and 15 illustrate the temperature dependent thermal conductivity of polyamide 11 with different loadings of multi-wall carbon nanotubes (MWNT) as a function of temperature and MWNT loading. The thermal conductivities were first measured at 40°C, then samples were heated to 175°C and measured. The thermal conductivities were then measured after the samples were cooled back to 40°C.

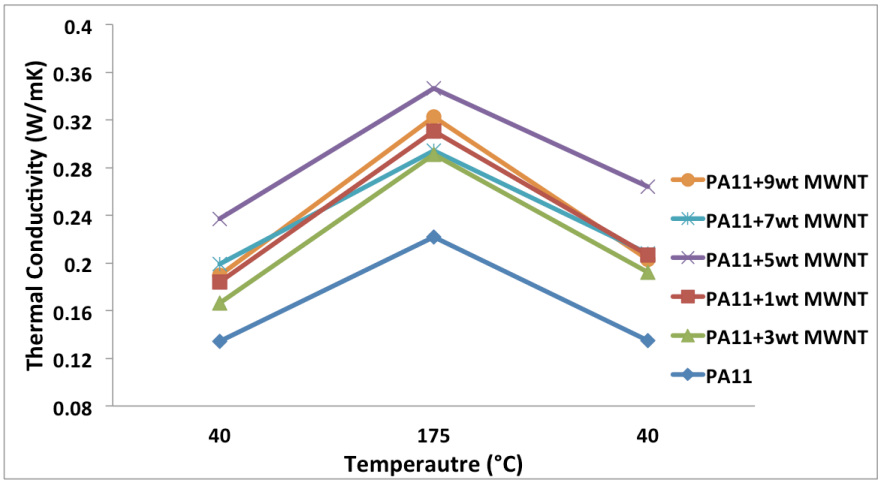

Figure 14： Temperature dependent thermal conductivity of fresh polyamide 11 with different loading of multi-wall carbon nanotubes as a function of temperature.

Figure 14 presents the experiment procedure that the loose powder was heated to 175°C then cooled down to 40°C. First the PA 11- MWNT nanocomposites thermal conductivity increased with the increasing temperature. Second the thermal conductivities of previously heated to 175°C nanocomposites at 40°C were 25% larger than that of fresh nanocomposites at 40°C. Third the thermal conductivity did not increase linearly with the MWNT loadings.

Figure 15: Thermal conductivity of polyamide 11-MWNT nanocomposites as a function of the weight fraction of the MWNT loadings.

Figure 15 shows that at each temperature, the thermal conductivity changed with the increasing MWNT loadings: a peak occurs at PA11- 5wt% MWNT blends; then thermal conductivity decreased at PA11- 3wt% MWNT blends and PA11- 7wt% MWNT blends. Moreover, thermal conductivity increased at PA11- 1wt% MWNT blends and PA11- 9wt% MWNT blends. In addition, Fig. 15 illustrates the fact that at the same MWNT loading, the thermal conductivities of previously heated to 175 °C nanocomposites at

40 °C are larger than that of fresh nanocomposites at 40 °C but smaller than the thermal conductivities of fresh nanocomposites at 175 °C.

Figures 16 and 17 show the SEM images of fresh PA11- 1wt% MWNT blends and PA11- 3wt% MWNT blends at 5,000 magnification. PA11-3wt% MWNT blend shows more and bigger agglomerates than PA11-1wt% MWNT blend.

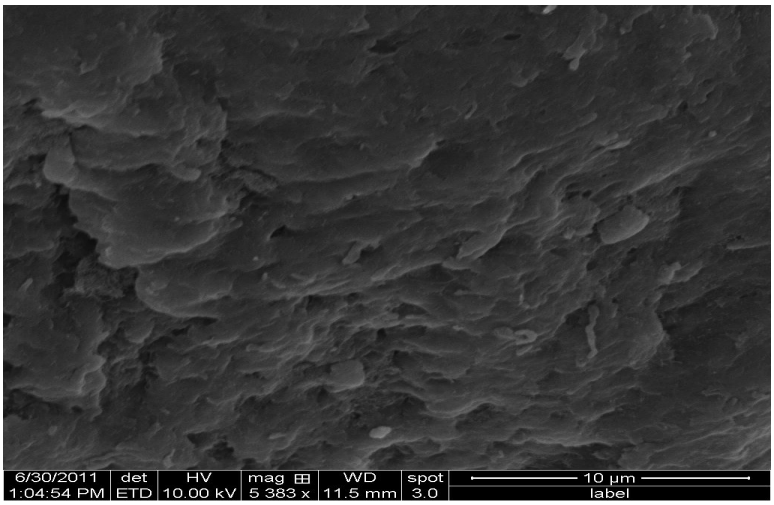

Figure 16: Surface view of PA11-1wt% MWNT at 5,000x.

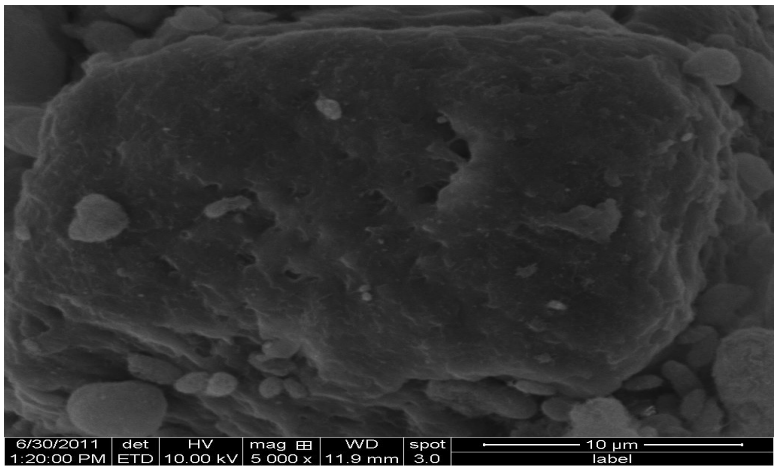

Figure 17: Surface view of PA11-3wt% MWNT at 5,000x.

Figures 18 and 19 show the SEM images of PA11- 5wt% MWNT blends at 5,000 and 40,000 magnifications. No large agglomerates were detected in Fig. 18. Figure 19 presents the well-dispersed surface view.

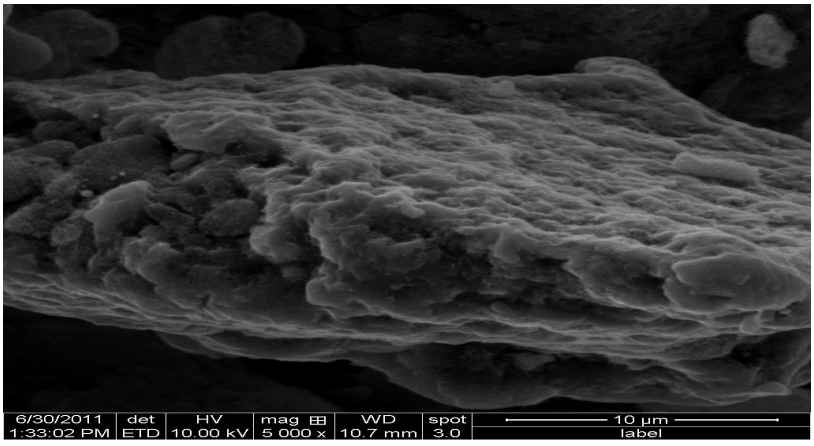

Figure 18: Surface view of PA11-5wt% MWNT at 5,000x.

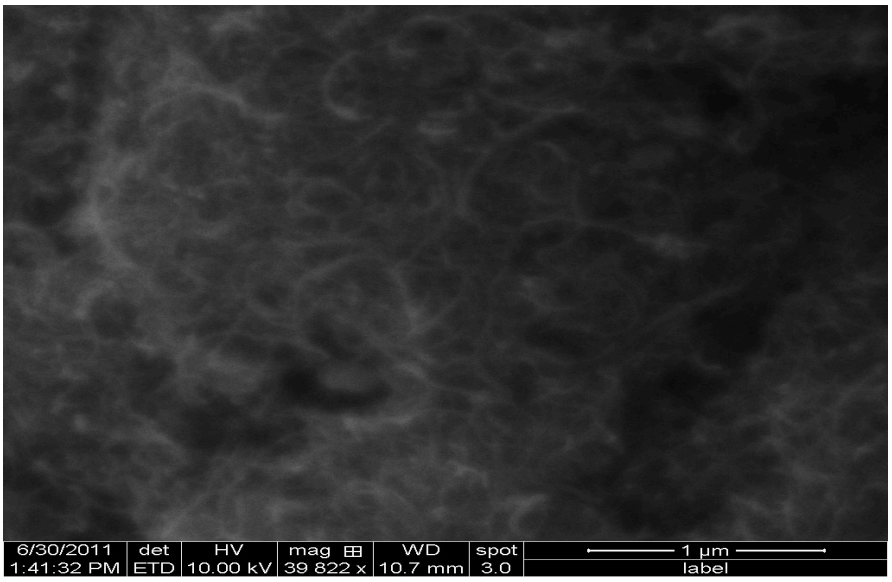

Figure 19: Surface view of PA11-5wt% MWNT at 40,000x.

Figures 20 and 21 show the SEM images of fresh PA11- 7wt% MWNT blends and PA11- 9wt% MWNT blends at 5,000 magnification. Both figures show MWNT agglomerates among the matrix.

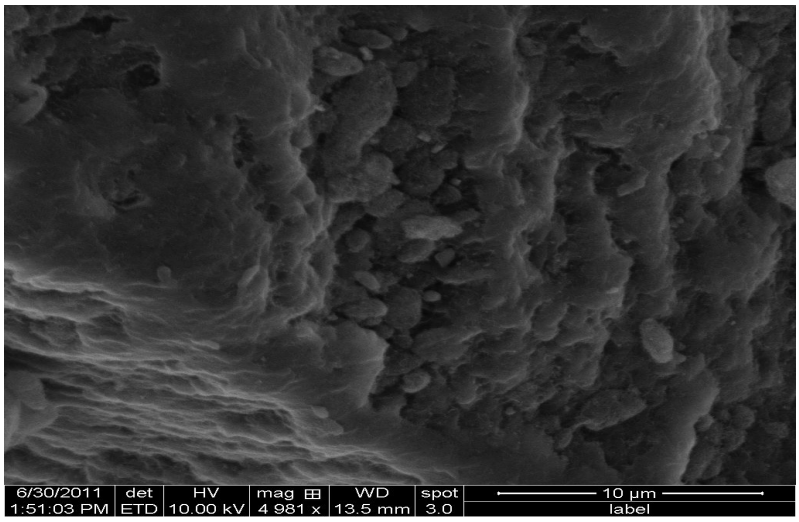

Figure 20: Surface view of PA11-7wt% MWNT at 5,000x.

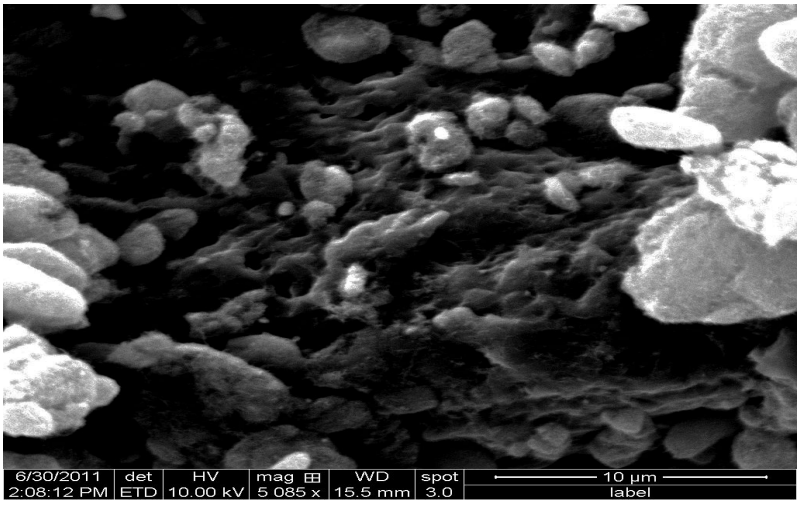

Figure 21: Surface view of PA11-9wt% MWNT at 5,000x.

Figure 22 shows the SEM image of previously heated to 175°C neat PA11 powder. Bridging was seen between the particles.

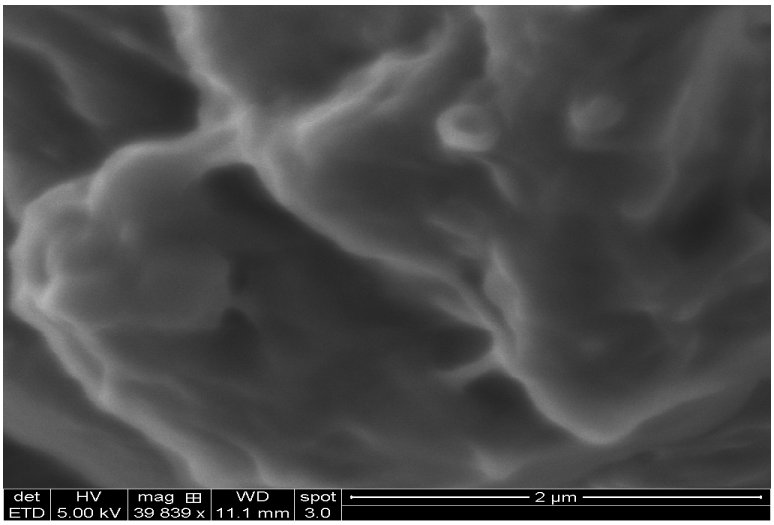

Figure 22: Surface view of neat previously heated PA 11 at 40,000x.

Chapter 4: *Discussion*

Chapter four analyzes the different effects of thermal conductivity measurements of polyamide. Comparisons are made between the theoretical data and the experimental results.

EFFECT OF POWDER BEHAVIOR AT DIFFERENT DENSITY

It is observed from the Figures 6 and 7 that at the same temperature, the thermal conductivity of fresh polyamide 12 increased with the increasing density. A linearized equation were obtained by the graph:

$$k = 0.0453*(T/T_{melt}) + 0.063*\Delta + 0.0317 \qquad [313\ K \leq T \leq 443\ K] \qquad (12)$$

where k is in units W/mK, Δ is the dimensionless relative density that equals ρ/ρ_{th}, where ρ_{th} is the full density of polyamide 12 powder 1.01 g/cc [19]. T is in units of Kelvin.

The slopes at different densities are the same, which indicates that the fresh powder temperature dependency is constant with density change. However, the starting point (thermal conductivity at 40 °C) increased with increasing density, which may be a result

of the geometry and the sample packing condition. Larger density means more particles in a constant volume.

Figure 23 includes a comparison of thermal conductivity results from the TPS 500 to Xue's experimental data [9].

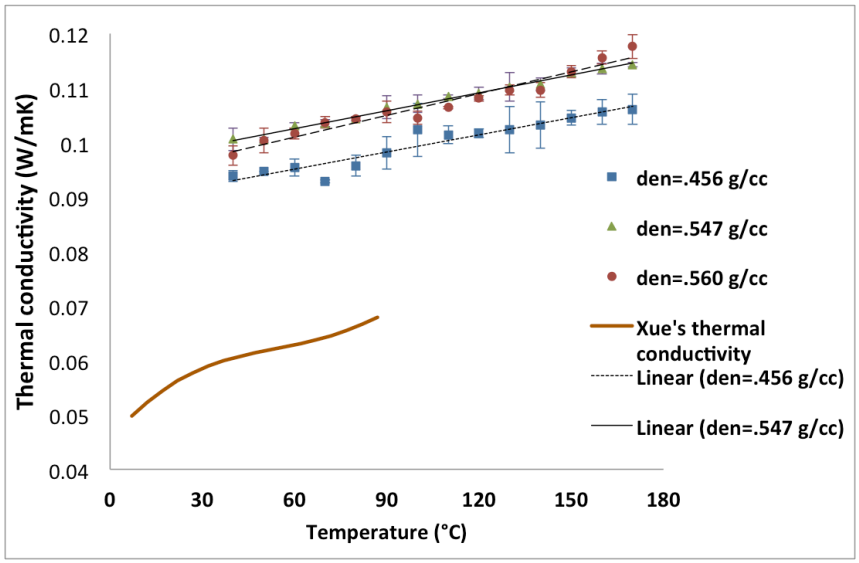

Figure 23: Comparison of thermal conductivity at three densities with Xue' s data [9].

A linearized equation were obtained from Xue's work:

$$k = 0.096*(T/T_{melt}) - 0.0032 \qquad [280 \leq T \leq 360] \qquad (13)$$

where k is in units W/mK, T is in units of Kelvin. Figure 23 and comparison of

Equation (13) with Equation (12) reveal that at each temperature, the experimental thermal conductivity results were larger than the results in Xue's work. In addition, the temperature dependent constant of Xue's work is twice as large as our experiment result. However, Xue did not mention the sample density and chemical makeup, and the temperature range was narrow.

Figure 24 presents an application of Saxena's model [8] using Equations (2), (3) and (4), which treated the natural loose and granular powder as a solid-gas mixture and separated the thermal conductivity calculation by porosity level.

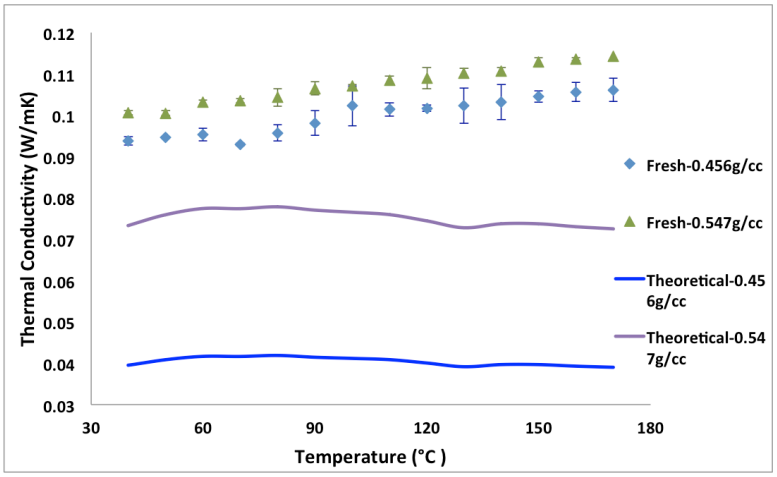

Figure 24: Comparison of thermal conductivity experiment results of polyamide 12 packed at 0.457 g/cc and 0.547 g/cc and Saxena's theoretical model [6].

Figure 24 shows at each density, Saxena's theoretical model data is 30%- 50% lower than experimental thermal conductivity results. It could due to the dependence on nitrogen thermal conductivity which is very low. The comparison of fresh polyamide 12 powder packed at 0.560 g/cc with the theoretical model is similar with that packed at 0.547 g/cc. Thermal conductivity of nitrogen (0.0256W/mK) was obtained from E.W. Lemmon and R.T. Jacobsen's work [20], which does not change much with increasing temperature.

Figures 25 and 26 show a comparison with Deissler and Boegli's maximum and minimum thermal conductivity model [12], Equations 7 and 8, respectively, with experimental measurements of the thermal conductivity of fresh polyamide 12 powder. Shown are the low and high packing density levels, 0.456 g/cc (Fig. 25) and 0.560 g/cc (Fig. 26). The results of the intermediate density, 0.547 g/cc, were similar to the values shown in Fig. 26.

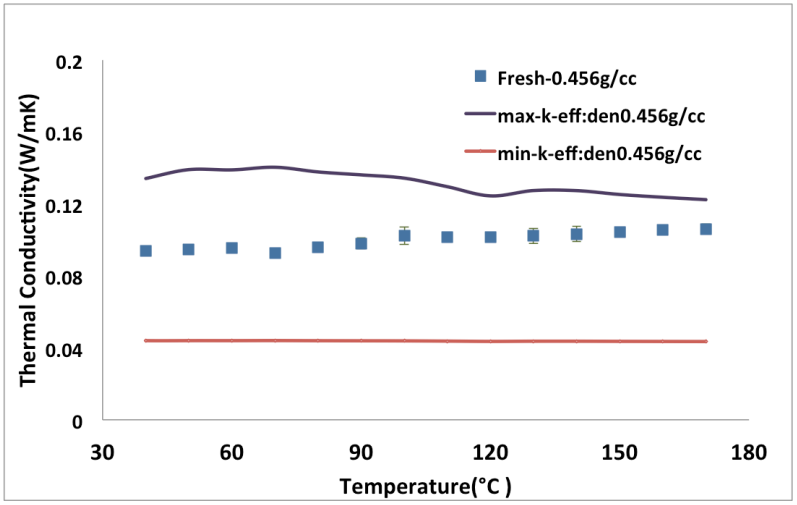

Figure 25: Comparison of thermal conductivity experiment results of polyamide 12 packed at 0.456 g/cc and Deissler and Boegli's theoretical model [12].

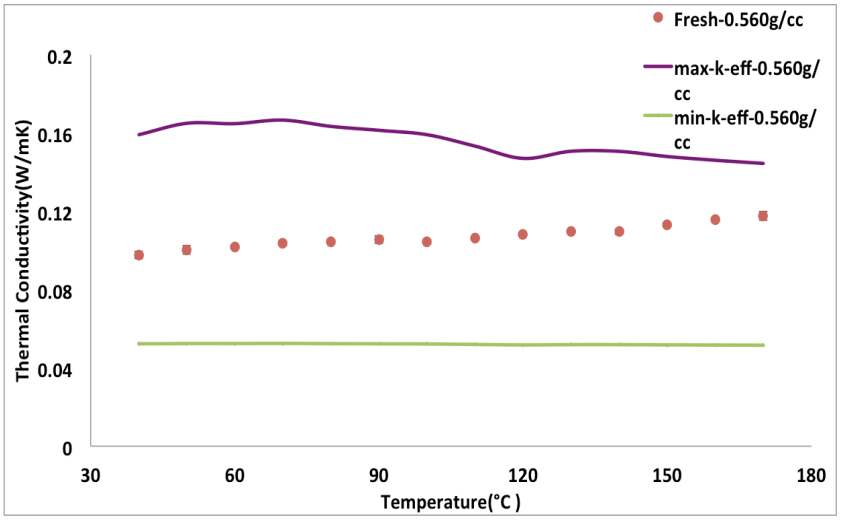

Figure 26: Comparison of thermal conductivity experiment results of polyamide 12 packed at 0.560 g/cc and Deissler and Boegli's theoretical model [12]. Comparison of polyamide 12 packed at 0.547 g/cc with the theoretical model is similar with Figure 26.

It is clearly seen that the experiment results fit well between the upper and lower limits. The thermal conductivity of nitrogen (0.0256W/mK) was obtained from E.W. Lemmon and R.T. Jacobsen's work [20].

Figure 7 indicates that the bulk laser sintered polyamide 12 cylinder had much higher thermal conductivity than loose powder. Thermal conductivity is dependent on the nature of inter-particle bonding, in that heat is conducted more easily through a polymer powder mass that is strongly bonded [21]. The solid sample had a more packed interior structure than the loose powder, so the thermal conductivity is significantly higher than that of the loose powder. Similarly, the thermal conductivity is higher for larger density samples.

However, the bulk polyamide showed a different trend compared to the loose powder. It reached a peak between 60°C and 80°C and then decreased constantly with increasing temperature. It is suggested that the polyamide molecular bonds were slightly weakened by increasing temperature, which reduced the effectiveness of the lattice to transmit phonons, the primary mechanism for thermal transport in polyamide. The thermal conductivity would thereby be lowered.

Regarding Figure 8, thermal conductivity of previously heated powder (mimicking laser sintered "powder cake") shows the same trend as the fresh powder: the curve for 0.547 g/ cc preheated polyamide 12 was close to that of 0.560 g/cc. Both curves showed constant higher values than the 0.456 g/cc specimen, but all maintained the same increasing trend. Mechanical bonds between individual contacting particles were strengthened during the initial heating process. This results in increased heat conduction through the polyamide powder mass on reheating. The maximum and minimum effective thermal conductivity theory [11] is also applied in this case, as shown in Fig. 27. The experimental results fit well with this theory.

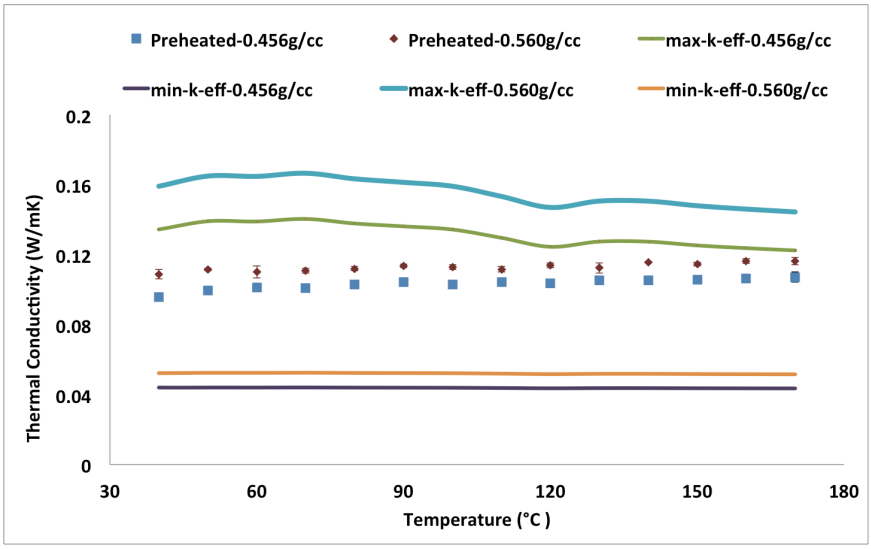

Figure 27: Comparison of thermal conductivity experiment results of polyamide 12 packed at 0.456 g/cc and 0.560 g/cc and Deissler and Boegli's theoretical model [12].

EFFECT OF PREHEATED POWDER

Figures 10 and 11 illustrate that at the same temperature, for different densities, 0.456 g/cc and 0.547 g/cc, preheated powder shows higher thermal conductivity than fresh powder, especially from 40 °C to 150 °C. This could be explained as due to improved interparticle bonding as the polyamide 12 powder cake was formed after reaching 170 °C. Adjacent powder particles adhere to each other, so the preheated powder had a higher thermal conductivity compared to fresh powder. The thermal conductivities for both are similar above 160°C. This may be explained that at high temperature close to the melting point, both forms of polyamide 12 are closely bonded.

Figure 11 illustrates the effect of powder caking on thermal conductivity of polyamide 12 at a density of 0.560 g/cc. The sample was removed from the powder holder after heating to 170 °C twice, crushed back to loose powder, packed in the sample holder and retested. The broken-up preheated powder line is similar with the fresh powder line, which shows a significantly different trend compared to the preheated powder line. From this, it is concluded that the increase in thermal conductivity is solely due to mechanical bonding of the particulate.

Two linearized relations were produced by regressing the data in Fig. 11 for the fresh powder, “part cake” (density= 0.560 g/cc):

$$k = 0.0453*T/T_{melt} + 0.0662 \quad \text{[fresh powder]} \tag{15}$$

$$k = 0.0453*T/T_{melt} + 0.0679 \quad \text{[”part cake”]} \tag{16}$$

where k is the thermal conductivity in W/mK and T is absolute temperature (K). The slight decrease in thermal conductivity of the crushed “part cake” is attributed to a lower relative density of the powder mass due to incomplete break-up of the bonded particulate. Deissler and Boegli’s theoretical effective thermal conductivity model [12] is applied and fits well to the polyamide12 powder that get through the preheat treatment, as shown in Fig. 28.

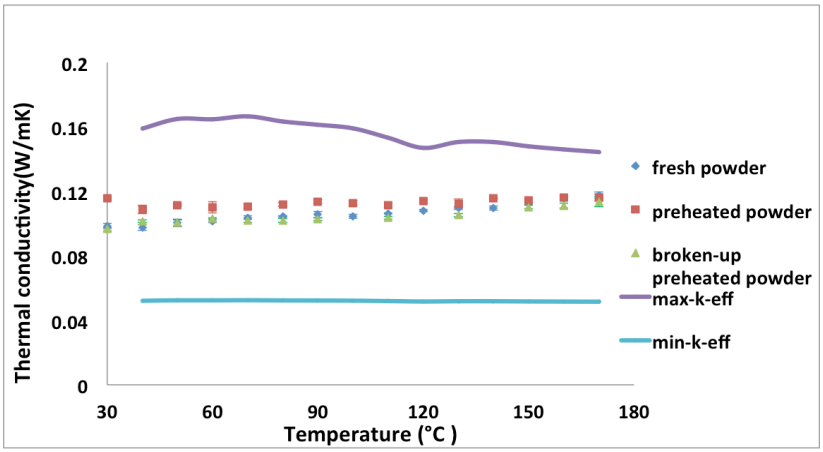

Figure 28: Application of Deissler and Boegli’s theoretical model [12] on broken-up previously heated to 170 °C polyamide 12 powder packed at 0.560 g/cc.

EFFECT OF TEMPERATURE ON POWDER CAKING

Figure 12 indicates that the polyamide 12 powder caked at a temperature between 160°C and 170°C. In the first four runs, thermal conductivity was linear with increasing temperature. However the fifth run presented 6 % higher thermal conductivity at 40°C, which is associated with the formation of powder cake. Based on a deviation from linearity on cooling, it is concluded that the powder begins to cake at approximately 170°C.

EFFECT OF CARRIER GAS

Figure 13 comprised two sets of experiment. One was charged with argon and the other was with nitrogen. It shows that the carrier gas did not influence the temperature dependent thermal conductivity. This is expected because first, both were athermic gases: thermal conductivities of nitrogen and argon are 0.02583 W/mK [18] and 0.016 W/mK [22], respectively. Second, the mass fraction of the carrier gas was low which led to very weak effect on porous sample performance. Deissler and Boegli's theoretical model [12] (Fig. 29) and Saxena's theoretical model [8] (Fig. 30) were applied below.

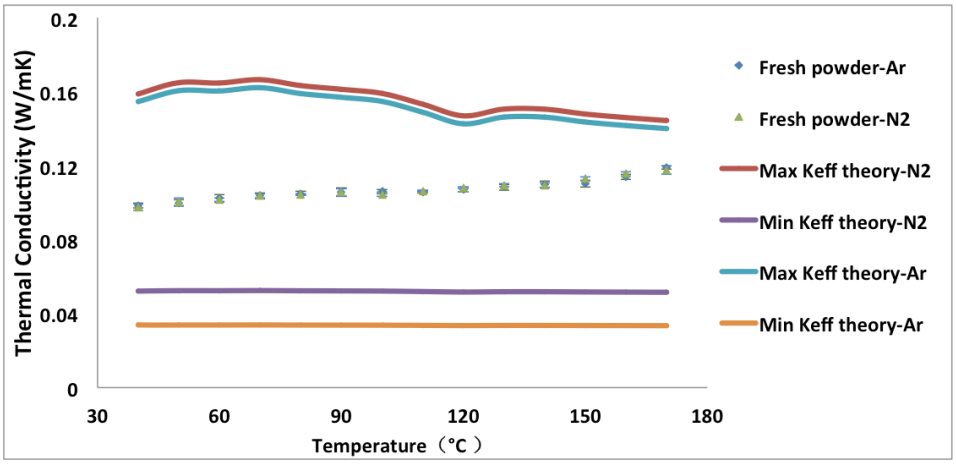

Figure 29: Comparison of thermal conductivity experiment results of polyamide 12 packed at 0.566 g/cc with different carrier gases (nitrogen and argon) and Deissler and Boegli's theoretical model [12].

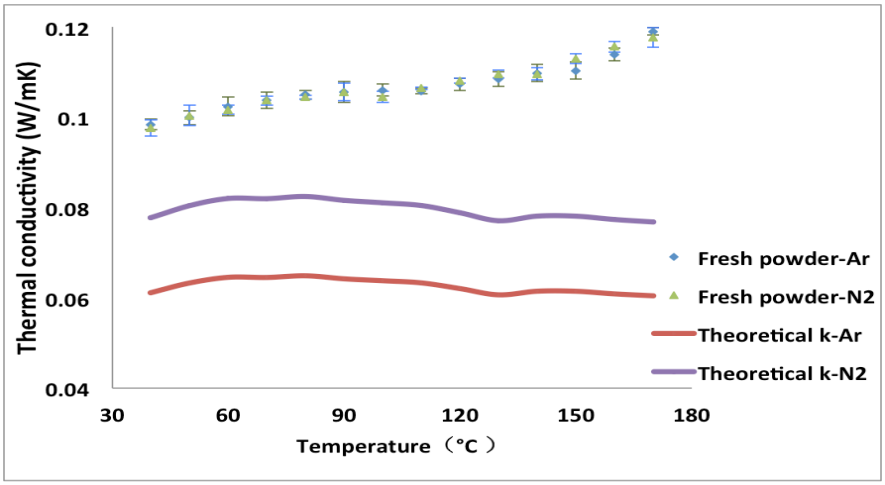

Figure 30: Application of Saxena's theoretical model [8] on thermal conductivity results of fresh polyamide 12 powder with argon or nitrogen packed at 0.560 g/cc.

Figure 29 illustrates that the thermal conductivity measurement results with different carrier gases fit the maximum and minimum effective thermal conductivity well. However, Saxena's theoretical model [8] shows lower thermal conductivity than experimental results. The reason could be the dependence on thermal conductivity of carrier gas during the effective thermal conductivity calculation. The carrier gas shares a quite small mass fraction in the solid-gas system, but it shares the equal importance with the solid in the effective thermal conductivity calculation.

EFFECT OF MWNT NANOCOMPOSITES

Since polyamide 11 shares similar physical, mechanical and chemical properties with polyamide 12, it was selected to blend with various multi-wall carbon nanotubes using powder- mixing technology to form nanocomposites. Figure 14 shows that the thermal conductivity of fresh polyamide 11 with multi-wall carbon nanotubes (MWNT) nanocomposites increased with the increasing temperature. The melting temperatures for each nanocomposite were between 185 °C and 205 °C, so the nanocomposites behaved in a semi-melting condition at 175 °C, and powder cake was formed. Thermal conductivity of previously heated to 175 °C nanocomposites at 40°C was larger than that of the fresh nanocomposites at 40 °C due to the strengthened mechanical bonds

during the heating process, but it is smaller than that of the fresh nanocomposites at 175 °C.

Regarding Fig. 15, in terms of fresh nanocomposties, at each temperature, PA 11- 5wt% MWNT blend shows the highest thermal conductivity. Figures 18 and 19 present surface view of PA 11- 5wt% MWNT blend under SEM, in which the PA11 and MWNT are well dispersed and no MWNT agglomerates were found. Besides that, thermal conductivity increases with the increasing MWNT loading at each temperature. Agglomerates were found in all other SEM images. Fig. 16 (PA 11- 1wt% MWNT) shows fewer agglomerates than Fig. 17 (PA 11- 3wt% MWNT) due to the less MWNT loading in the blends and the better dispersion condition, which results in larger thermal conductivity at each temperature. Fig. 20 (PA 11- 7wt% MWNT) and 21 (PA 11- 9wt% MWNT) all show MWNT agglomerates due to the increasing MWNT loading. Agglomeration prevents the effective heat conduction between particles and mechanical bonds were not strongly strengthened. It is therefore concluded that besides MWNT loading, agglomeration condition is the primary factor that influence the fresh PA11-MWNT nanocomposite thermal conductivity.

Figure 23 shows the SEM image of previously heated to 175°C neat PA 11 film. Bridging was found between the PA 11 particles, which enhanced the effective heat conduction path among particles and led to larger thermal conductivity.

Chapter 5: *Summary and Conclusions*

Polyamide 12 and polyamide 11 with different loading of MWNTs were analyzed in this thesis. There are several factors that attributed to the thermal conductivity change of polyamide according to this research.

SUMMARY

First, in loose powder form, thermal conductivity increased with the increasing temperature; however, in the bulk form, it decreased with increasing temperature.

Second, the thermal conductivity was proportional with the loose powder tapped density. The closer packed the sample is, the more particulate surfaces contacted other particles, which resulted in more heat transfer and a larger thermal conductivity.

Third, polyamide powder previously heated to 170°C shows constantly higher thermal conductivity than fresh powder, especially from temperatures ranging between 40°C to 150°C. Moreover, the crushed, preheated powder ("part cake") performed similarly to fresh powder. The experiment shows the powder caking temperature was approximately 170°C.

Fourth, the carrier gas, nitrogen or argon, did not influence on the thermal effect.

Last, thermal conductivity increased with the increasing loading of multi-wall carbon nanotubes (MWNT) in polyamide 11 blends.

CONCLUSIONS

Based on the summaries, several conclusions may be made:

- Thermal conductivity varies with powder packed density and temperature.
- Thermal conductivity of polyamide 12 in powder form is a third of that in bulk form.
- Inter-particle bonding is the primary factor that influences the polyamide 12 thermal conductivity.
- Fresh polyamide 12 powder cakes at around 170°C.
- Agglomeration condition is the primary factor that influences PA11- MWNT nanocomposites thermal conductivity.

Bibliography

[1] K.H. Tan, C. K. Chua, K.F. Leong, C.M. Cheah, P. Cheang, M.S. Abu Bakar,

[2]:K-Mac Plastics, 3821 Clay Ave. SW, Wyoming, MI 49548, available at: http://k-mac-plastics.net/index.htm.

[3] Dressler M, Rolling M, Schmidt M, Maturilli A, and Helbert J, 2010, "Temperature distribution in powder beds during 3D printing". *Rapid Prototyping Journal*, 16.

[4] M. Matsumoto, M. Shiomi, K. Osakada, F. Abe, 2002, "Finite element analysis of single layer forming on metallic powder bed in rapid prototyping by selective laser processing", *International Journal of Machine Tools & Manufacture*, pp. 61-67.

[5] S. Kolossov, E. Boillat, R. Glardon, P. Fischer, M. Locher, 2003, "3D FE simulation for temperature evolution in the selective laser sintering process". *International Journal of Machine Tools& Manufacture*, pp. 117-123.

[6] Rahul B. Patil, Vinod Yadava, 2007, “Finite element analysis of temperature distribution in single metallic powder layer during metal laser sintering”, *International Journal of Machine Tools & Manufacture. 47*, pp. 1069-1080.

[7] Nikolay K. Tolochko, Maxim K. Arshinov, Andrey V. Gusarov, Victor I. Titov, Tahar Laoui and Ludo Froyen, “Mechanisms of selective laser sintering and heat transfer in Ti powder”, 2003, *Rapid Prototyping Journal*, 9, pp. 314-326.

[8] Saxena, Chohan and Gustafsson, 1986, “Effective thermal conductivity of loose granular materials”, *J. Phys. D: Appl. Phys.19*, pp.1625-1630.

[9] Samuel Xue and J. W Barlow, 1990, “Thermal properties of powders”. In Solid Freeform Fabrication Proceedings. pp. 179-185.

[10] Dressler M, Rolling M, Schmidt M, Maturilli A, and Helbert J, 2010, “Temperature distribution in powder beds during 3D printing”. *Rapid Prototyping Journal*, 16.

[11] Fischer P, Karapatis N, Romano V, Glardon R, and Weber H, 2002. “A model for the interaction of near-infared laser pulses with metal powder in selective laser sintering”. *Applied Physics A: Materials Science and Processing*, 74(4), pp. 467-474.

[12] R. G. Deissler and J. S. Boegli, 1958. “An investigation of effective thermal conductivities of powders in various gases”. *Transactions of the ASME*, pp. 1417-1425.

[13] A.V. Gusarov, T. Laoui, L. Froyen, V.I. Titov, 2003. “Contact thermal conductivity of a powder bed in selective laser sintering”, *International Journal of Heat and Mass Transfer*, 46, pp. 1103-1109.

[14] A. J. Slavin, V. Arcas, C.A. Greenhalgh, E.R. Irvine, D. B. Marshall, 2002, “Theoretical model for the thermal conductivity of a packed bed of solid spheroids in the presence of a static gas, with no adjustable parameters except at low pressure and temperature”, *International Journal of Heat and Mass Transfer*, 45, pp. 4151-4161.

[15] Alan J. Slavin, Frank A. Londry, Joy Harrison, 1999, "A new model for the effective thermal conductivity of packed beds of solid spheroids: alumina in helium between 100 and 500 °C". *International Journal of Heat and Mass Transfer*, 43, pp. 59-73.

[16] T. Log and S.E. Gustafsson, 1995, "TPS technique for measuring thermal transport properties of building materials", *Fire and Materials*, Vol.19, pp. 43-49.

[17] Mark, J., 2007, Physical Properties of Polymers Handbook, Springer.

[18] Thermo.com, 2009, Pycnomatic ATC for solids and powders density specifications.

[19]: N. Ait hocine, P. Mederic, T. Aubry, 2008, "Mechanical properties of polyamide-12 layered silicate nanocomposites and their relations with structure", *Polymer Testing*, Volume 27, pp. 330-339.

[20] E. W. Lemmon and R. T. Jacobsen, 2004, 'Viscosity and thermal conductivity equaitons for nitrogen, oxgen, argon, and air', *International Journal of Thermophysics*, Vol. 25, pp. 21.

[21] "Engineering Plastics", 1985, ASM Engineered Materials Handbook , Volume 2, ASM Intl p. 60.

[22] The Engineering ToolBox, available at: http://www.engineeringtoolbox.com/thermal-conductivity-d_429.html.

Vita

Mengqi Yuan (Maggie) was born in China on November 8th, 1989. She studied Mechanical Engineering and Manufacturing in Huazhong University of Science and Technology in China for two years since 2006. Due to her excellent performance, she transferred to University of Birmingham in United Kingdom at 2008. She got two Bachelors' degrees (Hons.) in Mechanical Engineering at 2010. In August 2010, she entered the Graduate School at The University of Texas at Austin.

Maggie loves both classic and modern things. She loves playing piano, reading, high street fashion, and exploring new things.

Email: maggieyuanyuan1108@hotmail.com

This thesis was typed by Mengqi Yuan.